Journal of Engineering Science and Technology
Vol. 18, No. 3 (2023) 1650 - 1669

CAMPUS REOPENING DURING THE COVID-19: ODE-SIRD MODEL

SHAHIRAH ATIKAH MOHAMAD HUSNIN[1], NORAZALIZA MOHD JAMIL[2,*], KHAIRUL SALLEH ABDUL BASIT[3], NORYANTI MUHAMMAD[4]

[1,2,4]Centre for Mathematical Sciences, Universiti Malaysia Pahang, 26300 Gambang, Kuantan Pahang, Malaysia
[3]University Health Centre, Universiti Malaysia Pahang, 26300 Gambang, Kuantan, Pahang, Malaysia
[4]Centre of Excellence for Artificial Intelligence & Data Science, Universiti Malaysia Pahang, 26300 Gambang, Pahang, Malaysia
*Corresponding Author: norazaliza@ump.edu.my

Abstract

The education system went through major transformations and was adversely impacted when all schools and Higher Education Institutions (HEIs) were forced entirely to close due to the country dealing with the coronavirus disease 2019 (Covid-19) pandemic. This is now a phenomenon that significantly concerns people all over the world. Upon campus reopening, the outbreak will occur within the campus community, and the students might get infected. This paper proposed two types of mathematical models based on the Ordinary Differential Equation-Susceptible-Infected-Recovered-Dead (ODE-SIRD) framework to study the impact of campus reopening on the dynamic of the outbreak, which are: i) constant epidemiological parameters and ii) time-dependent epidemiological parameters. Other than that, a sensitivity analysis of parameters is carried out to determine the relative influence of the model parameters on disease transmission. We applied this model to observe Covid-19 cases in the selected higher institute in Malaysia. In comparison, the results indicate that the models with time-dependent rates better predict the progression of the Covid-19 outbreak. Hence, from this finding, the time-dependent function of epidemiological parameters should be included in a model for the Covid-19 outbreak related to campus reopening. The effect of lockdown time on the number of active cases is also investigated. In conclusion, the results help and improve in making a reasonable prediction about the infection's evolution of the outbreak.

Keywords: Campus reopening, Compartment model, Covid-19, Mathematical modelling, ODE, Sensitivity analysis, SIRD model.

1. Introduction

The Covid-19 outbreak in Wuhan, China, has affected many countries. This pandemic has affected people, including the economy, health, and education. According to United Nations Educational, Scientific and Cultural Organization (UNESCO) [1], more than 1.5 billion students were affected by the epidemic, particularly those in the youngest age range. Based on previous studies, closing education facilities is a viable option to break the transmission chain and reduce virus infection spread throughout the community [2, 3].

Many universities worldwide decided to cancel all campus gatherings, including face-to-face lectures, seminars, conventions, and other events, due to the growing concern over the spread of the Covid-19 pandemic. Furthermore, the university's management has been working hard to switch courses and services from the conventional delivery style (face-to-face) to online learning. For example, in China, the Ministry of Education migrated fully to online teaching and learning effectively on 4th February 2020 [4, 5]. As a result of the decision, institutions were asked to offer online courses with revised content and creative teaching techniques within a reasonably short period [5].

In the United States, about 400,000 cases of Covid-19 have been registered since the outbreak began in the spring of 2020. By the end of March, approximately 1,400 colleges and universities provided their courses to be online [6]. According to Kadvany [7], Stanford University and Touro College went fully online on 6th March 2020 to reduce the widespread of Covid-19. Moreover, more than half of all private, non-profit, and public universities announced their switch to online learning by the end of March [8].

In response to the Covid-19 outbreaks, The Ministry of National Education, Vocational Training, Higher Education, and Scientific Research in Morocco announced the closure of preschool and nursery schools, educational institutions, vocational training, managerial training, and universities on 13th March 2020 [9]. Other than that, Morocco's Ministry of Education has undertaken various remote education initiatives, including opening online university platforms and some television stations' involvement in broadcasting courses for rural regions with limited network access [9].

On the other hand, the Malaysian government took action and applied the first Movement Control Order (MCO) from 18th March 2020 until 31st March 2020. Subsequently, it continued from 1st April 2020 until 28th April 2020 to reduce the spread of the virus in the community [10, 11]. The MCO is known as lockdown, meaning mass gatherings in public places, such as religious services, were restricted. However, no interstate travel required the closure of all businesses except essential services, such as manufacturers, suppliers, retailers, and food outlets [12].

This lockdown has adversely impacted the education system as a temporary closure order has been issued for all educational institutions, including preschools, primary schools, secondary schools, colleges, and universities [12]. Due to the lockdown and quarantine, all physical learning and teaching were immediately replaced with virtual learning and teaching. The situation logically had the unintended consequence of negatively affecting the educational system, such as students who cannot cope with learning, are easily distracted, experience internet problems as students come from different areas, etc.

The decision to close the campus to avoid educational, mental, and financial problems is complicated because keeping the campus open would expose staff and students to a potentially fatal disease. Therefore, policymakers attempted to comprehend the risks associated with the gradual and total reopening. Nevertheless, a complete understanding of how the safety mechanism for reopening the campus works remains elusive. As a result, significant research effort in this area is required.

To better understand the characteristic of the Covid-19 outbreaks at a small residential college, Bahl et al. [13] created an agent-based model on a network. This indicates that strict regulation from the administration and students' careful behaviors are necessary for a successful campus reopening. A recent study by Frazier et al. [14] discovered that weekly asymptomatic screening of vaccinated undergraduates in Cornell's main campus gives considerable benefit against the Delta variation. They implemented a Susceptible, Exposed, Infectious, and Recovered (SEIR) model that ran with the age of those infected, symptom severity and intervention (testing, quarantine, and contact tracking) as the primary factors [14].

According to Bradley et al. [15], campus reopening approaches cannot be one-size-fits-all. Instead, well-planned colleges will implement various public health strategies perfectly suited to their resources, location, and culture. In other studies, Paltiel et al. [16] conclude that students must be tested every two days to open colleges safely, which is significantly more frequent than the current guidelines from the US Centers for Disease Control and Prevention. The crucial aspect for Bradley et al. [15] and Paltiel et al. [16], if the college cannot lower Covid-19 influx from outside and reproductive numbers ($R(t)$), more screening and a series of interlocking strategies are needed. This can isolate newly discovered patients within hours to prevent infection transmission and control outbreaks at a reasonable cost [17].

Given the current situation with the Covid-19 outbreaks, universities in Malaysia must reopen safely. In this paper, we aim to develop and simulate the outbreak of Covid-19 based on the impact of campus reopening on the dynamic outbreak. We focused on constructing a time-varying parameters compartmental model to stimulate the number of Covid-19 cases due to campus reopening and lockdown measures and the associated basic reproduction number (R_0). To do this, we used a compartment model of the Susceptible-Infected-Recovered-Dead (SIRD) model with two different parameters, i) constant epidemiological parameters and ii) time-dependent epidemiological parameters. Correspondingly, these two models were coded in MATLAB, and these results were compared. Furthermore, a sensitivity analysis of the epidemiological system is calculated to determine how important the model parameters are to the spread of the disease. Apart from that, the developed model was tested using the actual data of Covid-19 cases affecting staff and students at the selected higher institute in Malaysia from 4th October 2021 until 16th December 2021, and the results are discussed. Lastly, the study's conclusion is provided in the last section of the paper.

2. Mathematical Modelling

Various mathematical models were utilized to study the dynamic of the outbreak associated with campus reopening: deterministic, stochastic, and phenomenological. For example, Linka et al. [18] adopted a network SEIR model to simulate the return of all undergraduate students at Stanford University, US. They review three different scenarios: the actual infection dynamics under the wild-type

SARS-CoV-2 and the hypothetical outbreak dynamics under the new Covid-19 variants B.1.1.7 and B.1.351 with 56% and 50% increased exposure, respectively [18]. Other than that, their study reveals that even minor exposure changes can significantly impact overall case numbers. Furthermore, their findings recommend that population mixing raises the risk of local outbreaks, especially as new and more infectious variants emerge worldwide.

Lopman et al. [6] developed an SEIR compartment transmission model of how SARS-CoV-2 spreads among students, staff, and faculty at Emory University, an average-sized university. They explored a probabilistic sensitivity analysis on various screening and testing frequencies. They discovered that the community-introduced SARS-CoV-2 infection on campus could be monitored through effective testing, isolation, contact tracing, and quarantine. This is compatible with findings that this strategic approach has been effective in the general population when applied correctly.

In another study, Andersen et al. [19] employed statistical analysis to investigate the relationship between US college reopening and changes in human mobility on campus. To estimate the daily reproductive numbers ($R(t)$), a Bayesian approach was implemented. Their study presents how people and groups move and mix when colleges close and reopen due to a pandemic. It also provides strategic tools for analyzing the benefits and costs of school reopening and closing policies.

We applied a SIRD compartment model to describe the outbreak of Covid-19 in certain higher learning institutes due to the impact of campus reopening, which is an extension of the Susceptible-Infected-Recovered (SIR) model proposed by Kermack and McKendrick in 1927 [20, 21]. In this compartment model, population size is supposed to be fixed and constant during the epidemic. This model divided the population into four groups: susceptible (S), infected (I), recovered (R), and dead (D).

The SIRD compartment model consists of the following:

$S(t)$: The total number of people that potentially become infected with the diseases from day 1 to day t.
$I(t)$: The total number of infected people by the disease from day 1 to day t.
$R(t)$: the total number of people who recovered from the disease from day 1 to day t.
$D(t)$: The total number of people who died directly from the disease from day 1 to day t.

Suppose that the total population impacted by the pandemic is denoted as N. Therefore, the equation of population is represented as follows:

$$N(t) = S(t) + I(t) + R(t) + D(t) \tag{1}$$

The outbreaks were modeled using the following conditions: the total population of the higher learning is constant. Furthermore, we assumed that N is the number of students returning to campus (N = the sum of the number of students returning to the campus). This implies that the birth and death rates are the same over the relevant time [22, 23]. Moreover, the I people come into close contact with the S people (sporadic cases not linked to other clusters are not considered) [23].

Considering the conditions, the SIRD model is described by the set of ODE as follows:

$$\frac{dS}{dt} = -\beta \frac{1}{N} S(t) I(t), \tag{2}$$

$$\frac{dI}{dt} = \beta \frac{1}{N} S(t)I(t) - \gamma I(t) - \mu I(t), \quad (3)$$

$$\frac{dR}{dt} = \gamma I(t), \quad (4)$$

$$\frac{dD}{dt} = \mu I(t), \quad (5)$$

where infection rate (β) is defined as the rate of infection growth, recovered rate (γ) represents the population increases of the recovering population, and the death rate (μ) represents the growth rate of the deceased population.

Equation (2) demonstrates how the number of *S* populations changes over time. The equation represents negative as the number of *S* will decrease if the population comes into close contact with infectious people, and they would get infected. The first term of the right-hand side (RHS) of Eqs. (2) and (3) represented an output value for the *S* population and an input value for the *I* population [23]. For Eq. (3), the number of *I* individuals might be lowered if they recovered (group *R*) or died (group *D*), as shown in Eqs. (4) and (5), respectively [23]. Note that Eqs. (4) and (5) displayed how the number of people who *R* and the number of people whom *D* changed over time.

The equilibrium point (S^*, I^*) is obtained by solving,

$$\frac{dS}{dt} = -\beta \frac{1}{N} S(t)I(t) = 0,$$

$$\frac{dI}{dt} = \beta \frac{1}{N} S(t)I(t) - \gamma I(t) - \mu I(t) = 0,$$

$$\frac{dR}{dt} = \gamma I(t) = 0 \text{ and}$$

$$\frac{dD}{dt} = \mu I(t) = 0,$$

which implies $I^* = 0$ and infinitely many solutions for S^*. Therefore, the equilibrium points of this model is $(S^*, I^*) = (S^*, 0)$.

Consequently, we estimated the R_0 of this model by applying the next-generation matrix method proposed by Van Den Driessche and Watmough [24]. Here, R_0 is defined as the number of secondary infections caused by a single infected person in a susceptible population [25, 26]. First, we need to construct the next-generation matrix of the epidemic by determining which compartment in the set of ODE describes the emergence of new infections and the evolution of the epidemic among infected individuals. This refers to the infected compartment in Eq. (3).

Suppose $\mathcal{F}(I) = \frac{\beta SI}{N}$ and $\mathcal{V}(I) = (\gamma + \mu)I$. The R_0 is the spectrum of FV^{-1}, where,

$$F = \frac{\partial \mathcal{F}}{\partial I} = \frac{\beta S}{N}$$

and

$$V = \frac{\partial \mathcal{V}}{\partial I} = \gamma + \mu.$$

At equilibrium point $(S^*, I^*) = (S^*, 0)$ and assuming $S^* = N$, we obtained $F = \beta$ and $V = \gamma + \mu$. Hence, $FV^{-1} = \frac{\beta}{(\gamma+\mu)}$. Therefore,

$$R_0 = \frac{\beta}{(\gamma+\mu)}. \tag{6}$$

In this paper, we proposed two models called Models I and II, where in Model I, β, γ, and μ are set to be constants. On the other hand, Model II formulated β, γ, and μ as time-dependent functions. Constant epidemiological parameters, also known as time-independent parameters, were employed in many studies [3, 27-29]. However, this model has some limitations, such as its inability to include the influence of effective measures. Previous studies have reported that parameter-varying modifications of the SIRD compartment model can define various stages of the transmission of Covid-19. For example, Calafiore et al. [27] implemented the modelling of Covid-19 in Italy with parameter-varying models to consider probable variations in epidemic behaviour, such as those caused by containment measures imposed by authorities or changes in epidemic features, as well as the influence of enhanced antiviral therapy.

Alternatively, Wang et al. [3] separated the period into four phases, resulting in piecewise constant parameters to estimate the Covid-19 outbreaks in China. There are also some studies on time-dependent parameters, such as a time-dependent SIR model developed to track the transmission rate and recovery rate to predict the number of infected individuals at a certain time [28]. Likewise, Keller et al. [29] constructed a novel Bayesian time-varying coefficient state-space model for infectious disease transmission to investigate the influence of population mobility on the spread of Covid-19. Their models study how mobility affected the transmission of Covid-19 outbreaks in several United States and Colorado counties.

Hence, to better understand the transmission of Covid-19 due to the campus reopening, we implemented the parameter variation over time depending on the lockdown date and reopening. The period was split into two phases as follows:

Phase 1: From day 1 until the lockdown, $t < t_{lockdown}$

Phase 2: After the campus lockdown, $t \geq t_{lockdown}$

The model utilized here is the modified model presented in Caccavo [22], Mohd Jamil et al. [23] and Jamil and Gill [30] which is based on the SIRD compartment model. Let day 1 be on 4th October 2021 with the data obtained from the institute's health office. Subsequently, the higher institute implemented the lockdown on 13th November 2021 (day 41), calculated from day 1st to 4th of October 2021, denoted as $t_{lockdown}$.

Model II is formulated as follows:

$$\beta(t) = \begin{cases} \beta_1 t + \beta_2, & t < t_{lockdown} \\ \beta_0 exp\left(-\frac{(t-t_{lockdown})}{\tau_\beta}\right), & t \geq t_{lockdown} \end{cases}, \tag{7}$$

$$\gamma(t) = \begin{cases} \gamma_2 t + \gamma_3, & t<t_{lockdown} \\ \gamma_0 + \frac{\gamma_1}{1+\exp(-t+t_{lockdown}+\tau_\gamma)}, & t\geq t_{lockdown} \end{cases}, \tag{8}$$

$$\mu(t) = \begin{cases} \mu_2 t + \mu_3, & t < t_{lockdown} \\ \mu_0 exp\left(-\frac{(t-t_{lockdown})}{\tau_\mu}\right) + \mu_1, & t \geq t_{lockdown} \end{cases}. \tag{9}$$

From Eq. (7) in Phase 1, it is assumed that the infection rate, $\beta(t)$ is a linear function, where individuals in the community were free to move around when the outbreak started. This is also applicable to recovery rate ($\gamma(t)$) and death rate ($\mu(t)$) as displayed in Eqs. (8) and (9). When the lockdown was implemented (Phase 2), people were isolated and physically separated from one another. Thus, this phenomenon was represented by an exponential decay function in Eqs. (7) and (9). After the lockdown, the function decreases exponentially as people are separated from one another (reduction of β) and, in particular, for groups that are most at risk of death (reduction of μ). After the lockdown, the recovery rate was represented by a logistic function in Eq. (8) as the infected people got treatment, leading to a higher γ. From Eqs. (7)-(9), τ_β represents the characteristic time of transmission rate, the characteristic time of recovery rate denotes as τ_γ and τ_μ is the characteristic time of death rate.

The following set of initial conditions is required to solve a 4-set ordinary Eqs. (2)-(5):

$$S(0) = N - I(0) + R(0) + D(0),\ I(0) = 8,\ R(0) = 2,\ D(0) = 0. \tag{10}$$

These initial conditions were obtained from the collected data by the institute health center on 4th October 2021. The 14 unknown parameters ($\beta_0, \beta_1, \beta_2, \tau_\beta, \gamma_0, \gamma_1, \gamma_2, \gamma_3, \tau_\gamma, \mu_0, \mu_1, \mu_2, \mu_3, \tau_\mu$) were applied in Model II. The system of the ordinary equation from Eqs. (2)-(5) and (7)-(9) was constructed into MATLAB using the 4th-order Runge-Kutta method and parameter fitting techniques. Apart from that, the value of unknown parameters was first gained using the gradient-free algorithm (pattern search). Other than that, pattern search methods are direct search methods that are effective in improving an initial approximation and locating the neighbourhood of a local solution [31, 32]. Torczon [33] presented that "pattern search" techniques applied to a general smooth function in n dimensions converge to a stationary point. Subsequently, the obtained root mean square error (RMSE) between the real data and model was further minimized by the Nelder-Mead algorithm. Note that the Nelder-Mead algorithm is a method for minimizing a real-valued function [31]. This algorithm is a local search method that is the most widely employed to solve parameter estimation and unconstrained optimization problems [24, 26]. This study used these two algorithms to reach the global minima by getting the unknown parameters.

3. Results and Discussion

Following Malaysia's Covid-19 outbreak, the government decided to implement the MCO on 18th March 2020. Almost all sectors, including education, have been closed due to the MCO, as universities and other educational institutions in Malaysia have been affected by this policy as of March 2020. Until January 2021, the situation in Malaysia is still in the state of Conditional Movement Control Order (CMCO) and Rehabilitation Movement Control Order (RMCO).

On 14th September 2021, the Ministry of Higher Education (MOHE) announced the opening of HEIs for the physical admission of students for the 2021/2022 Academic Session [34]. However, the reopening of the universities only involved fully vaccinated students and academic and non-academic staff to create safe campus bubbles. Following that, the physical admission of students to campus began on 15th October 2021. This admission will take place in stages along with the guidelines and Standard Operational Procedure (SOP) through the coordination of the HEIs to provide a safe campus community when it reopens [34]. Therefore, Table 1 contains a summary of the operation of HEIs beginning on 15th October 2021.

Table 1. Summary of the operation of HEIs.

No.	Operation of Higher Education Institutions (HEIs)
1	Admission of fully vaccinated students to the HEIs involves all categories of students and all phases of the National Rehabilitation Plan (NRP), with priority given to students in need.
2	Admissions to the HEIs will be implemented in stages from 15th October 2021, according to the academic calendar of the respective institutes. Therefore, HEIs need careful planning by identifying students, determining the movement schedule, and ensuring that students undergo strict health screening.
3	The admission process for these students will employ the HEIs' SOP. Therefore, strict SOPs must be followed for mobility to be controlled.
4	Entrance to the campus is restricted to only those students, academic staff, and non-academic staff who have been vaccinated with a full dose injection of the vaccine and have passed the period of effectiveness after vaccination.
5	Only a letter of approval from the Institution to return to campus is required for Institutions in the Peninsula.
6	Students in Sarawak, Sabah, and Labuan must undergo Covid-19 Screening (RT-PCR swab test) and get a cross-district/cross-state authorization letter from the police.
7	In order to effectively handle symptomatic cases or infections, HEIs need to establish isolation facilities within their institutions.
8	The fee reduction of 20% for all citizen students at public universities for Semester 1 Session 2021/2022 benefited 555,340 students with a total value of RM175 million.
9	Students may choose to continue their learning by online classes in their localities for courses or programs offered online. In addition, activities involving laboratories, workshops, and research can be carried out in groups under the direction of specified SOPs.
10	Admission of international students from the UK., Mobility, and Edu tourism program students and dependents with valid visas may enter Malaysia.

On 16th September 2021, the selected HEIs are preparing to accept physical admission of students to the campus starting on 15th October 2021. This involves a group of students who need to return to the campus and those who have previously completed the vaccination. Following the announcement made by the MOHE, it would be implemented in stages for the campuses.

The HEI has identified 6334 students from the category of students who need to return to campus, including the final-year students who must return to campus by the stated deadline. In addition, beginning on 15th October 2021, teaching and learning activities will be delivered in a hybrid format (online and face-to-face) according to the needs of the program study. Therefore, the university has also strengthened the campus's SOP by requiring that campus residents complete their vaccination to form safe campus bubbles.

Meanwhile, the HEI has increased its efforts to contact students who have not yet received vaccines and encouraged them to visit a vaccination centre near their homes to receive injections to be allowed to enter the campus. As a result, the institute's health center data presents that 5892 students from 13 states and 3 federal territories in Malaysia have returned to the campus. Other than that, the higher learning institute has allowed some categories of students to return to the campus following the dates, i) 15th-17th October 2021, ii) 22nd-24th October 2021, and iii) 29th-31st October 2021.

Table 2 represents the number of students from different states and federal territories, showing that students from Selangor have the highest number of returned to campus compared to other states, followed by Pahang.

Table 2. Number of students returning to campus on 15th - 31st October 2021 from 13 states and 3 federal territories in Malaysia.

State	No of students	State	No of students
Johor	569	Pulau Pinang	172
Kedah	373	Sabah	288
Kelantan	738	Sarawak	176
Melaka	186	Selangor	977
Negeri Sembilan	252	Terengganu	604
Pahang	907	Putrajaya	24
Perak	393	Wilayah Persekutuan	194
Perlis	25	Labuan	14

Based on the institute's health center data, the number of daily Covid-19 cases before the campus reopening was below 10. During the first three days of the campus reopening, on the 15th, 16th, and 17th of October 2021, the number of daily Covid-19 cases was 7, 8, 9, respectively. After six days after the first stages of campus reopening, the number of positive cases increased to two-digit: 13 cases. However, following the return of all students to campus, the number of daily Covid-19 infections remained in double digits, below 20 cases.

Note that Malaysia celebrated Deepavali on 3rd November 2021. As the holidays fall on Thursday, most students and staff who did not have classes on Friday got to extend their holiday by combining it with a weekly holiday on Saturday and Sunday. As a result of the relatively long four-day holidays, many students could travel to their hometowns. Therefore, Covid-19 cases spiked after the holiday due to the movement of entering and existing students and staff to the campus. The number of Covid-19 cases increased to 23 after a week of the Deepavali holiday. Based on the report from the health office of the institute, on 12th November 2021, there was a Covid-19 outbreak of 27 positive cases in the institute.

After 28 days of the campus reopening, the daily positive cases in the higher learning institute show an increasing number. Due to this, the mobility of students entering and exiting the campus was controlled and prohibited following Administrative Circular No. 11, the Year 2021, issued on 12th November 2021. Following that, all physical interaction activities on the campus, including teaching and learning, were not allowed, and the entire campus was monitored and controlled by the Institute Security Division.

Hence, the total lockdown at the campus is effective immediately from 13th November 2021 until 26th November 2021. In addition, the university has also decided that students must do Test, Report, Isolate, Inform, and Seek (TRIIS) to regulate and prevent infection and Covid-19 transmission on campus as an additional control strategy. The timeline of the campus reopening and campus lockdown is shown in Table 3.

Table 3. The timeline of campus reopening and campus lockdown.

Date	Description of the campus reopening and campus lockdown
15/10/2021 (Campus reopen)	MOHE announced that the physical admission of students to campus would begin on 15th October 2021. This admission will take place in stages along with the guidelines and SOP through the coordination of the HEIs to provide a safe campus community when it reopens. Following that, there were 5892 students from different states, and the federal had returned to the campus in stages.
13/11/2021 (Campus lockdown)	After 28 days of reopening, the HEI indicates increasing positive cases. Due to this, the university implemented a total lockdown on campus for about 14 days. Further to this announcement, all staff needed to work from home, and all physical classes were shifted to online learning.
27/11/2021 (Campus reopen after the lockdown)	The campus reopened back as usual with no notice for further lockdown. The number of daily cases shows slightly decreased after the lockdown. All physical interaction activities on campus are carried out in stages.

Figure 1 demonstrates the graph of actual data of the positive number of Covid-19 in the higher learning institute obtained from the health office. The graph below illustrates the data from 4th October 2021 until 16th December 2021. The figure illustrates that the number of infected cases on the campus keeps increasing after the campus reopens on 15th October 2021. According to data obtained from the health center of the institute, on 13th November 2021, which is the first day of lockdown, the number of infected cases was 37. It is the highest number after 28 days of campus reopening. During the 7th day of lockdown, the number of infected cases rose to 46.

After 14th days of lockdown, the number of infected cases slowed down to 18 cases. The number of infected cases then slowed down until the middle of December. This indicates that cases significantly decrease when the lockdown is implemented. However, it takes about 14 days to see the impact of the lockdown on the reduced number of cases.

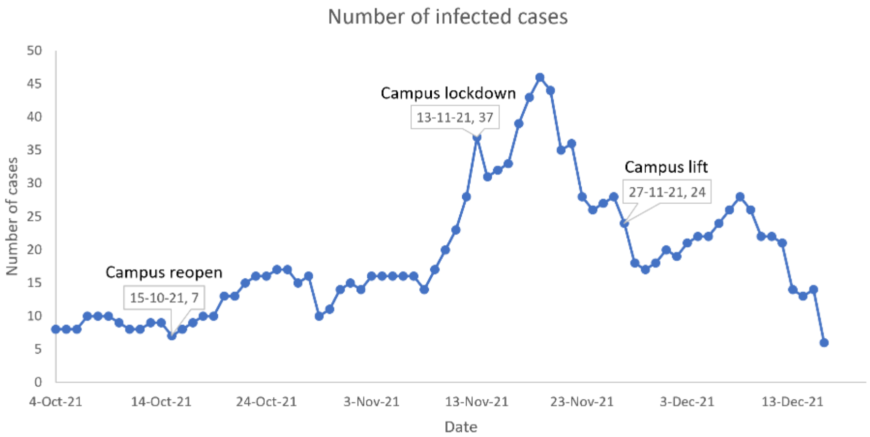

Fig. 1. Number of infected cases on the campus.

Figure 2 shows the graph of the fitted model with the collected data in the higher learning institute, representing (a) Model I and (b) Model II. In the graph, the actual data is denoted by an asterisk symbol, and lines represent the SIRD model.

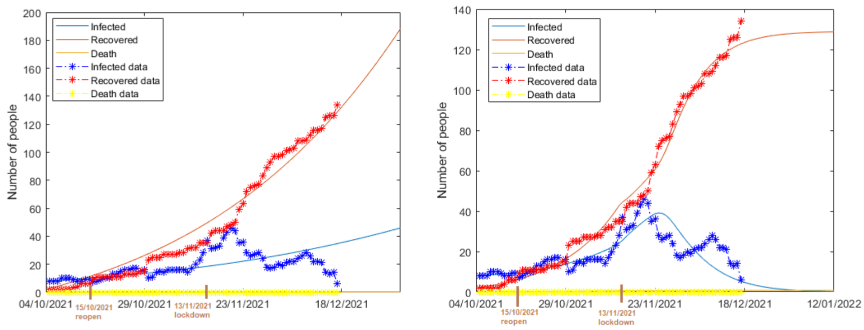

(a) Model I **(b) Model II**

Fig. 2. SIRD Model based on data from the higher learning institute.

Based on Fig. 2(a), the yellow line, which represents the death compartment, fits well with the obtained data. However, the R compartment (red line) and I compartment (blue line) does not resemble the actual data trend. Based on Fig. 2(b), the R compartment (red line) and D compartment (yellow line) are well-fitted to the observed data. Note that the graph for the R compartment denotes a slightly different pattern at the end of the model from the actual data, as the model predicted that the R compartment might require more time to reach its maximum point before remaining constant. It is also shown that the I compartment (blue line) predicted that the cases would rise later than the actual data. Overall, the R and I compartments for Model II provide a much better fit compared to Model I.

The 4th-order Runge-Kutta method is used to numerically solve the system of ODEs in Eqs. (2)-(5) and (7)-(9). In order to make the model work, it is necessary to estimate solving and assign values to each of the model's parameters [35]. Hence, the numerical method was embedded with parameter fitting techniques and coded in MATLAB for Models I and II. For Model I, the obtained values of β, γ, and μ were shown in Table 4.

Table 4. Value of parameter for Model I.

No.	Parameters	Value
1	β	0.1137
2	γ	0.0924
3	μ	0.0001

Based on Table 4, β presents the highest value compared to the γ rates and μ rates. Meanwhile, there were 14 parameters utilized in Model II. The values of the 14 unknown parameters were tabulated in Table 5.

Based on Table 5, the characteristic time of transmission rate, τ_β shows the highest number compared to τ_γ and τ_μ. The higher the τ_β, the longer the time required to reduce the number of cases.

Table 5. Value of 14 parameters determined by parameter fitting techniques.

No.	Parameters	Value	No.	Parameters	Value
1	β_0	0.1238	8	γ_3	0.0000
2	β_1	0.0029	9	τ_γ	11.8014
3	β_2	0.0269	10	μ_0	0.0000
4	τ_β	22.1588	11	μ_1	0.0002
5	γ_0	0.0548	12	μ_2	0.0021
6	γ_1	0.0869	13	μ_3	0.0006
7	γ_2	0.0396	14	τ_μ	23.4237

Sensitivity analysis of each parameter, which is related to the R_0 is determined in this part. The sensitivity analysis reveals the significance of each disease transmission parameter [36]. Therefore, understanding the link between input and output variables allows us to assess the relative change in a variable when a parameter changes [37, 38]. As there are typical mistakes in data collection and assumed parameter values, sensitivity analysis is frequently performed to test the robustness of model predictions to parameter values [37].

The positive index for the index of model parameters related to the R_0 indicates that there is a direct relationship between the parameters and the R_0 [39]. The negative sensitivity index indicates that increased R_0 have a negative significance. In other words, changes to this parameter while other parameters remain constant will lead to a decrease in the R_0 [39].

Using Eq. (6), $R_0 = \frac{\beta}{(\gamma+\mu)}$ is a theoretical formulation for the sensitivity of R_0 that can be achieved concerning each parameter in Table 5. The resulting parameter values are presented in Table 6. The formula for sensitivity analysis of R_0 that depends differentially on a parameter p is given by:

$$Y_p^{R_0} = \frac{\partial R_0}{\partial p} \times \frac{p}{R_0}. \tag{11}$$

Phase I: Before lockdown (let $t = 40$).

$$R_0 = \frac{\beta_1 t+\beta_2}{\gamma_2 t+ \gamma_3+\mu_2 t+\mu_3}.$$

Consider the sensitivity for parameter β_1,

$$Y_{\beta_1}^{R_0} = \frac{\partial R_0}{\partial \beta_1} \times \frac{\beta_1}{R_0} = \frac{t}{\gamma+\mu} \times \frac{\beta_1(\gamma+\mu)}{\beta_1 t+\beta_2} = \frac{\beta_1 t}{\beta_1 t+\beta_2} = 0.81176.$$

Consider the sensitivity for parameter β_2,

$$Y_{\beta_2}^{R_0} = \frac{\partial R_0}{\partial \beta_2} \times \frac{\beta_2}{R_0} = \frac{1}{\gamma+\mu} \times \frac{\beta_2(\gamma+\mu)}{\beta_1 t+\beta_2} = \frac{\beta_2}{\beta_1 t+\beta_2} = 0.18824.$$

Consider the sensitivity for parameter γ_2,

$$Y_{\gamma_2}^{R_0} = \frac{\partial R_0}{\partial \gamma_2} \times \frac{\gamma_2}{R_0} = \frac{\beta}{(\gamma_2 t+ \gamma_3+\mu)^2} \times t \times \frac{\gamma_2(\gamma_2 t+ \gamma_3+\mu)}{\beta} = 0.99994.$$

Consider the sensitivity for parameter γ_3,

$$Y_{\gamma_3}^{R_0} = \frac{\partial R_0}{\partial \gamma_3} \times \frac{\gamma_3}{R_0} = \frac{\beta}{(\gamma_2 t+ \gamma_3+\mu)^2} \times \frac{\gamma_3(\gamma_2 t+ \gamma_3+\mu)}{\beta} = 0.$$

Consider the sensitivity for parameter μ_2,

$$Y_{\mu_2}^{R_0}=\frac{\partial R_0}{\partial\,\mu_2}\times\frac{\mu_2}{R_0}=\frac{\beta}{(\gamma+\mu_2t+\mu_3)^2}\times t\times\frac{\mu_2(\gamma+\mu_2t+\mu_3)}{\beta}=0.47458.$$

Consider the sensitivity for parameter μ_3,

$$Y_{\mu_3}^{R_0}=\frac{\partial R_0}{\partial\,\mu_3}\times\frac{\mu_3}{R_0}=\frac{\beta}{(\gamma+\mu_2t+\mu_3)^2}\times\frac{\mu_3(\gamma+\mu_2t+\mu_3)}{\beta}=0.00339.$$

Phase II: After lockdown (let $t=41$).

$$R_0=\frac{\beta_0 exp\left(-\frac{(t-41)}{\tau_\beta}\right)}{\left(\gamma_0+\frac{\gamma_1}{1+\exp(-t+41+\tau_\gamma)}\right)+(\mu_0 exp\left(-\frac{(t-41)}{\tau_\mu}\right)+\mu_1)}.$$

Consider the sensitivity for parameter β_0,

$$Y_{\beta_0}^{R_0}=\frac{\partial R_0}{\partial\beta_0}\times\frac{\beta_0}{R_0}=\frac{exp\left(-\frac{(t-41)}{\tau_\beta}\right)}{\gamma+\mu}\times\frac{\beta_0(\gamma+\mu)}{\beta_0 exp\left(-\frac{(t-41)}{\tau_\beta}\right)}=1.$$

Consider the sensitivity for parameter τ_β,

$$Y_{\tau_\beta}^{R_0}=\frac{\partial R_0}{\partial\tau_\beta}\times\frac{\tau_\beta}{R_0}=-\frac{(t-41)}{(\tau_\beta)^2}\times -exp\left(-\frac{(t-41)}{\tau_\beta}\right)\times\frac{\tau_\beta}{exp\left(-\frac{(t-41)}{\tau_\beta}\right)}=\frac{(t-41)}{\tau_\beta}=0.$$

Consider the sensitivity for parameter γ_0,

$$Y_{\gamma_0}^{R_0}=\frac{\partial R_0}{\partial\gamma_0}\times\frac{\gamma_0}{R_0}=-\frac{\beta}{(\gamma_0+\frac{\gamma_1}{1+\exp(-t+41+\tau_\gamma)}+\mu)^2}\times\frac{\gamma_0(\gamma_0+\frac{\gamma_1}{1+\exp(-t+41+\tau_\gamma)}+\mu)}{\beta}=-0.99635.$$

Consider the sensitivity for parameter γ_1,

$$Y_{\gamma_1}^{R_0}=\frac{\partial R_0}{\partial\gamma_1}\times\frac{\gamma_1}{R_0}=-\frac{\beta\left(1+\exp(-t+41+\tau_\gamma)\right)}{(\gamma_0+\gamma_1+\mu)^2}\times\frac{\gamma_1(\gamma_0+\gamma_1+\mu)}{\beta\left(1+\exp(-t+41+\tau_\gamma)\right)}=-0.61240.$$

Consider the sensitivity for parameter τ_γ,

$$Y_{\tau_\gamma}^{R_0}=\frac{\partial R_0}{\partial\tau_\gamma}\times\frac{\tau_\gamma}{R_0}=-\frac{\beta}{\left(\gamma_0+\frac{\gamma_1}{1+\exp(\tau_\gamma)}+\mu\right)^2}\times-\frac{\gamma_1(\exp(\tau_\gamma))}{\left(1+\exp(\tau_\gamma)\right)^2}\times\frac{\tau_\gamma\left(\gamma_0+\frac{\gamma_1}{1+\exp(\tau_\gamma)}+\mu\right)}{\beta}=0.00013.$$

Consider the sensitivity for parameter μ_0,

$$Y_{\mu_0}^{R_0}=\frac{\partial R_0}{\partial\mu_0}\times\frac{\mu_0}{R_0}=\frac{\beta(exp\left(-\frac{(t-41)}{\tau_\mu}\right))}{\left(\mu_1+\mu_0 exp\left(-\frac{(t-41)}{\tau_\mu}\right)+\gamma\right)^2}\times\frac{\mu_0(\mu_1+\mu_0 exp\left(-\frac{(t-41)}{\tau_\mu}\right)+\gamma)}{\beta}=0.$$

Consider the sensitivity for parameter μ_1,

$$Y_{\mu_1}^{R_0}=\frac{\partial R_0}{\partial\mu_1}\times\frac{\mu_1}{R_0}=-\frac{\beta}{\left(\mu_0 exp\left(-\frac{(t-41)}{\tau_\mu}\right)+\mu_1+\gamma\right)^2}\times\frac{\mu_1\left(\mu_0 exp\left(-\frac{(t-41)}{\tau_\mu}\right)+\mu_1+\gamma\right)}{\beta}=-0.00364.$$

Consider the sensitivity for parameter τ_μ,

$$Y_{\tau_\mu}^{R_0}=\frac{\partial R_0}{\partial\tau_\mu}\times\frac{\tau_\mu}{R_0}=\frac{\beta\mu_0 exp\left(-\frac{(t-41)}{\tau_\mu}\right)}{\left(\mu_0 exp\left(-\frac{(t-41)}{\tau_\mu}\right)+\mu_1+\gamma\right)^2}\times-\frac{(t-41)}{(\tau_\mu)^2}\times\frac{\tau_\mu\left(\mu_0 exp\left(-\frac{(t-41)}{\tau_\mu}\right)+\mu_1+\gamma\right)}{\beta}=0.$$

Therefore, the results of the sensitivity index of model parameters were tabulated in Table 6.

Table 6. Sensitivity index of model parameters related to basic reproduction number.

No.	Parameters	Value	No.	Parameters	Value
1	γ_0	-0.99635	8	τ_γ	0.00013
2	γ_1	-0.61240	9	μ_3	0.00339
3	μ_1	-0.00364	10	β_2	0.18824
4	γ_3	0.00000	11	μ_2	0.47458
5	μ_0	0.00000	12	β_1	0.81176
6	τ_β	0.00000	13	γ_2	0.99994
7	τ_μ	0.00000	14	β_0	1.00000

The sensitivity index in Table 6 displays the parameter with the lowest sensitivity followed by the highest one. The highest sensitivity index is β_0, and followed by γ_2, β_1, μ_2, and so on. Based on Table 6, most of the parameters of the ODE-SIRD model have a positive sensitivity index, while three parameters whose γ is (γ_0, γ_1) and death rate is (μ_1) has a negative sensitivity index. On the other hand, γ_3, μ_0, τ_β and, τ_μ have zero value of sensitivity index, meaning that the model is unaffected by changes in the parameter's value. Parameters of Phase I (before lockdown) consist of β_1, β_2, γ_2, γ_3, μ_2, μ_3 whereas β_0, τ_β, γ_0, γ_1, τ_γ, μ_0, μ_1, τ_μ relate to Phase II (after lockdown).

Parameter of recovery rate after lockdown (γ_0 , γ_1) presents a negative sensitivity index towards R_0 compared to the parameter of γ before lockdown (γ_2, γ_3). A negative value of sensitivity analysis means that if the parameters are raised, then the R_0 goes lower. This means that the higher the γ after the lockdown, the lower the spread of the disease in the population. Based on Table 6, it is clear that the parameters τ_γ, μ_3, β_2, μ_2, β_1, γ_2 increase the value of R_0 and increase the epidemic. Hence, in this model, the most sensitive parameter for R_0 is the parameter for β (β_0, β_1, β_2), as the value for the parameter before and after lockdown gave the positive value of sensitivity analysis.

The performance of the compartment model for Models I and II were compared based on their RMSE, as shown in Table 7. From the results, the proposed model in this study, denoted as Model II, has a lower RMSE value than Model I. It presents that the time-dependent functions improved the fit of the SIRD model compared to the constant parameter in Model I. Note that the RMSE values for the proposed function of this model quantify that the model is close to the regression line compared to the constant function because of the lower value of the RMSE values.

Table 7. Comparison of the RMSE using two different models for the Covid-19 outbreaks.

Model	RMSE
Model I	1.0816×10^4
Model II	0.4365×10^4

Hence, the graph of Model II exhibited a better prediction than Model I. This concluded that the time-dependent function for epidemiological parameters gave a better result than constant parameter values.

Figure 3 portrays the simulation study of the effect of different lockdown times on the cumulative number of Covid-19 infected cases ($t_{lockdown}$= 41, 61, 81). Other than that, the additional simulation is carried out if the $t_{lockdown}$ was delayed and changed to 3rd December 2021 (day 61) and 23rd December 2021 (day 81), which was calculated from day 1 on 4th October 2021. Referring to the figure, $t_{lockdown}$= 41 is the actual lockdown time imposed on 13th November 2021, with a maximum peak of 28 cases on 15th November 2021. If $t_{lockdown}$= 61 and $t_{lockdown}$= 81, the maximum peak is 72 cases (5th December 2021) and 218 cases (25th December 2021), respectively. Based on the results obtained, a delay in the lockdown will delay the reduction of the infected cases. The graph for $t_{lockdown}$=81 indicates a significant rise in the infected cases. This clearly indicates that if the lockdown were delayed and postponed, the number of infected cases would keep increasing. Therefore, the cumulative number of infected cases took a long time to reduce, which led to a longer lockdown period.

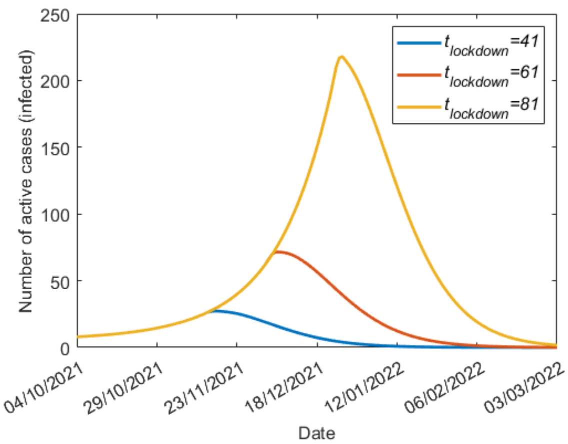

Fig. 3. The effect of lockdown time on the number of active cases at the selected higher institute.

Significant delays in lockdown lead to a rapid increase in cumulative cases. As a result, it is essential to consider the timing of the lockdown relative to the number of cases in controlling the pandemic in communities. Earlier lockdowns reduce the spread of Covid-19 in communities, where significant delays result in a rapid increase in cases. The delay in the lockdown will also make the Covid-19 outbreak more difficult to control as it peaks and overstressed the healthcare providers. Other than that, the lockdown implementation (administratively) has significantly improved, preventing the virus from spreading from one person to another. The sensitivity index concerning the ODE-SIRD model parameters shows that the parameters β_0, β_1, β_2, γ_2, μ_2, μ_3, and τ_γ increase the value of R_0 which in turn increases the epidemic. Therefore, the parameters with a negative sensitivity index will decrease the epidemic.

4. Conclusions

In this study, we discussed and compared two ODE-SIRD models for the outbreak of Covid-19 due to the campus reopening for selected HEIs in Malaysia. Our model with time-dependent epidemiological parameters predicts better than the constant parameter. Moreover, this proved that a parameter-varying modification of the SIRD compartment model described and predicted the behavior of the Covid-19 outbreaks well. Based on the result, the effect of the lockdown after campus reopening can be seen after 14 days. However, significant delays in lockdown caused a rapid increase in the total number of cases, which took longer to reduce. Consequently, it is essential to consider the timing of the lockdown relative to the number of cases controlling the pandemic in communities. This model could help provide insight into the dynamic of the spread of Covid-19 with the effect of campus reopening, in which the university management/authority could plan more efficiently and effectively to flatten the curve at the university level.

Moreover, we estimated the R_0, and carried out a sensitivity analysis of the R_0 to identify the relative significance of the model parameters in disease transmission. Based on the result obtained, the sensitivity analysis indicates that the infection transmission rate before and after the lockdown implementation plays a significant role in the spread of disease. This is because the most sensitive parameter in this compartment model was the β ($\beta_0, \beta_1, \beta_2$). This enables us to identify to which our model's predictions hold up under different settings, how well the model predicts outcomes related to parameter values, and how each parameter affects the disease's basic reproduction rate. Other than that, this analysis can provide essential information to decision-makers who may be confronted with the reality of an infectious disease.

Acknowledgement:

This research is supported by the Ministry of Higher Education under the Fundamental Research Grant Scheme (FRGS) No. FRGS/1/2021/STG06/UMP/02 /3 (University reference RDU210122). The authors would like to thank Ts. Dr. Azlyna binti Senawi for many fruitful discussions on the situation of Covid-19 pandemic in the selected higher institute.

Nomenclatures

β	Rate of infection growth
γ	Rate of recovered
μ	Rate of death
τ_β	The characteristic time of transmission rate
τ_γ	The characteristic time of recovery rate
τ_μ	The characteristic time of death rate

Abbreviations

Covid-19	Coronavirus Diseases 2019
HEIs	Higher Education Institutions
MOHE	Ministry of Higher Education
ODE	Ordinary Differential Equation
RMSE	Root Mean Square Error
SIRD	Susceptible Infected Recovered Dead
SOP	Standard Operational Procedure
WHO	World Health Organization

References

1. UNESCO (2020). COVID-19 impact on education. Retrieved January 7, 2023, from https://en.unesco.org/covid19/educationresponse.

2. Kawano, S.; and Kakehashi, M. (2015). Substantial impact of school closure on the transmission dynamics during the pandemic flu H1N1-2009 in Oita, Japan. *PLoS One*, 10(12), 1-15.
3. Wang, H.; Wang, Z.; Dong, Y.; Chang, R.; Xu, C.; Yu, X.; . Zhang, S.; Tsamlag, L.; Shang, M.; Huang, J.; Wang, Y.; Xu, G.; Shen, T.; Zhang, X.; and Cai, Y. (2020). Phase-adjusted estimation of the number of coronavirus disease 2019 cases in Wuhan, China. *Cell Discovery*, 6(1), 1-8.
4. Ministry of Education. (2020). Introduce the relevant situation of online education in primary and secondary schools during the epidemic and the consideration of the next step. Retrieved January 7, 2023, from http://www.moe.gov.cn/fbh/live/2020/51987/mtbd/202005/t20200518_455656.html.
5. Xinhua. (2020). Chinese universities to remain closed until effective control of epidemic. Retrieved January 9, 2023, from http://www.xinhuanet.com/english/2020-02/25/c_138814715.htm.
6. Lopman, B.; Liu, C.Y.; Le Guillou, A.; Handel, A.; Lash, T.L.; Isakov, A.P.; and Jenness, S.M. (2021). A modeling study to inform screening and testing interventions for the control of SARS-CoV-2 on university campuses. *Scientific Reports*, 11(1), 1-11.
7. Kadvany, E. (2020). Stanford tells 7,000 undergraduates to leave campus: class will be online only next quarter. Retrieved January 5, 2023, from https://paloaltoonline.com/news/2020/03/06/stanford-cancels-in-person-classes-two-students-possibly-exposed-to-coronavirus-in-self-isolation.
8. Lu, H.; Weintz, C.; Pace, J.; Indana, D.; Linka, K.; and Kuhl, E. (2021). Are college campuses superspreaders? A data-driven modeling study. *Computer Methods in Biomechanics and Biomedical Engineering*, 24(10), 1136-1145.
9. Draissi, Z.; and ZhanYong, Q. (2020). COVID-19 outbreak response plan: Implementing distance education in Moroccan Universities. Retrieved June 5, 2022, from https://ssrn.com/abstract=3586783.
10. Aw, S.B.; Teh, B.T.; Ling, G.H.T.; Leng, P.C.; Chan, W.H.; and Ahmad, M.H. (2021). The covid-19 pandemic situation in Malaysia: Lessons learned from the perspective of population density. *International journal of Environmental Research and Public Health*, 18(12), 6566.
11. Khor, V.; Arunasalam, A.; Azli, S.; Khairul-Asri, M.G.; and Fahmy, O. (2020). Experience from Malaysia during the COVID-19 movement control order. *Urology*, 141, 179-180.
12. Tamin, N.H.; and Mohamad, M. (2020). Google Classroom for teaching and learning in Malaysia primary school during movement control order (MCO) due to Covid19 pandemic: A literature review. *International Journal of Multidisciplinary Research and Publications*, 3(5), 34-37.
13. Bahl, R.; Eikmeier, N.; Fraser, A.; Junge, M.; Keesing, F.; Nakahata, K.; and Reeves, L. (2021). Modeling COVID-19 spread in small colleges. *Plos One*, 16(8), e0255654.
14. Frazier, P.I.; Cashore, J. M.; Duan, N.; Henderson, S.G.; Janmohamed, A.; Liu, B.; Shmoys, D.B.; Wan, J.; and Zhang, Y. (2022). Modeling for COVID-19 college reopening decisions: Cornell, a case study. *Proceedings of the National Academy of Sciences*, 119(2), e2112532119.

15. Bradley, E. H.; An, M. W.; and Fox, E. (2020). Reopening colleges during the coronavirus disease 2019 (COVID-19) pandemic-one size does not fit all. *JAMA Network Open*, 3(7), e2017838-e2017838.
16. Paltiel, A. D.; Zheng, A.; and Walensky, R. P. (2020). Assessment of SARS-CoV-2 screening strategies to permit the safe reopening of college campuses in the United States. *JAMA Network Open*, 3(7), e2016818-e2016818.
17. Opatowski, L.; Guillemot, D.; Boëlle, P.Y.; and Temime, L. (2011). Contribution of mathematical modeling to the fight against bacterial antibiotic resistance. *Current opinion in Infectious Diseases*, 24(3), 279-287.
18. Linka, K.; Peirlinck, M.; Schäfer, A.; Tikenogullari, O. Z.; Goriely, A.; and Kuhl, E. (2021). Effects of B. 1.1. 7 and B. 1.351 on COVID-19 dynamics: A campus reopening study. *Archives of Computational Methods in Engineering*, 28(6), 4225-4236.
19. Andersen, M. S.; Bento, A. I.; Basu, A.; Marsicano, C.; and Simon, K. (2021). College openings, mobility, and the incidence of COVID-19 cases. Retrieved June 3, 2022, from https://doi.org/10.1101/2020.09.22.20196048.
20. Kermack, W.O.; and McKendrick, A.G. (1932). Contributions to the mathematical theory of epidemics. II.-The problem of endemicity. *Proceedings of the Royal Society of London. Series A, containing papers of a mathematical and physical character*, 138(834).
21. Wearing, H.J.; Rohani, P.; and Keeling, M.J. (2005). Appropriate models for the management of infectious diseases. *PLoS Medicine*, 2(8), e174.
22. Caccavo, D. (2020). Chinese and Italian COVID-19 outbreaks can be correctly described by a modified SIRD model. Retrieved June 1, 2022, from https://doi.org/10.1101/2020.03.19.20039388.
23. Mohd Jamil, N.; Rosli, N.; and Muhammad, N. (2022). Simulation of COVID-19 outbreaks via Graphical User Interface (GUI). *Journal of Public Health Research*, 11(1), jphr-2021.
24. Van den Driessche, P.; and Watmough, J. (2002). Reproduction numbers and sub-threshold endemic equilibria for compartmental models of disease transmission. *Mathematical Biosciences*, 180(1-2), 29-48.
25. Siettos, C.I.; and Russo, L. (2013). Mathematical modelling of infectious disease dynamics. *Virulence*, 4(4), 295-306.
26. Wang, P. C.; and Shoup, T. E. (2011). Parameter sensitivity study of the Nelder-Mead simplex method. *Advances in Engineering Software*, 42(7), 529-533.
27. Calafiore, G.C.; Novara, C; and Possieri, C. (2020). A time-varying SIRD model for the COVID-19 contagion in Italy. *Annual Reviews in Control*, 50, 361-372.
28. Chen, Y.C.; Lu, P.E.; Chang, C.S.; and Liu, T.H. (2020). A Time-dependent SIR model for COVID-19 with undetectable infected persons. *IEEE Transactions on Network Science and Engineering*, 7(4), 3279-3294.
29. Keller, J.P; Zhou, T.; Kaplan, A.; Anderson, G.B.; and Zhou, W. (2022). Tracking the transmission dynamics of COVID-19 with a time-varying coefficient state-space model. *Statistics in Medicine*. 41(15), 2745-2767.
30. Jamil, N.M.; and Gill, B.S. (2022). Estimation of Public Compliance with COVID-19 Prevention Standard Operating Procedures Through a

Mathematical Model. *Proceedings of 2nd International Conference on Mathematical Modeling and Computational Science*, *(ICMMCS)*, Singapore, 49-58.

31. Lagarias, J.C.; Reeds, J.A.; Wright, M.H.; and Wright, P.E. (1998). Convergence properties of the Nelder--Mead simplex method in low dimensions. *SIAM Journal on optimization*, 9(1), 112-147.
32. Lewis, R.M.; Torczon, V.; and Trosset, M.W. (1998). Why pattern search works. *Institute for Computer Applications in Science and Engineering, NASA Langley Research Center,* 59(1998), 1-7.
33. Torczon, V.J. (1989). *Multi-directional search: a direct search algorithm for parallel machines.* Ph.D. Thesis, Department of Computational & Applied Mathematics, Rice University .
34. Badra. (2021). IPT akan dibuka semula bagi pembelajaran fizikal bermula Oktober 2021. Retrieved May 23, 2022, from https://harianpost.my/ipt-dibuka-semula-oktober-2021/.
35. Mekonen, K.G.; H/Michael, T.G.; and Feyissa, S. (2020). Parameter estimation of COVID-19 pandemic model with self protection behavior changes. Retrieved January 7, 2023, from https://doi.org/10.1101/2020.08.24.20180695.
36. Rodrigues, H.S.; Monteiro, M.T.T.; and Torres, D.F.M. (2013). Sensitivity analysis in a dengue epidemiological model. *Conference Papers in Mathematics*, 2013, 1-7.
37. Affi, P.O. (2019). Global stability analysis of the SEIR deterministic model in the presence of treatment at the latent period. *Mathematics Letters*, 4(4), 67-73.
38. Rangkuti, Y.M.; and Landong, A. (2022). Sensitivity analysis of SEIR epidemic model of Covid 19 spread in Indonesia. *Proceedings of the 3rd International Conference on Sciences and Technology Applications (ICOSTA), Medan, Indonesia,* 012092.
39. Rampal, L.; and Liew, B.S. (2021). Malaysia's third COVID-19 wave-a paradigm shift required. *The Medical Journal of Malaysia*, 76(1), 1-4.

Appendix A

Computer Programme

A. 1. Programme Structure and Description of Subroutines

MATLAB programming language is used in programming the prediction models. The main flow chart of the programme is shown in Figure A-1.

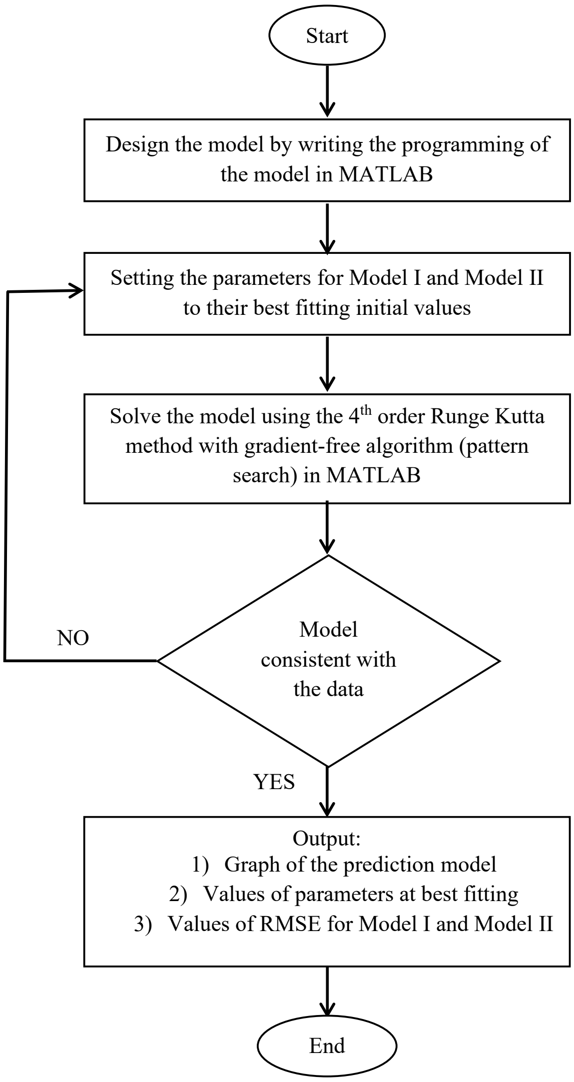

Fig. A-1. Main flow chart of the computer programme used in this study.